

# Ratiometric Detection of Adenosine-5'-triphosphate (ATP) and Cytidine-5'-triphosphate (CTP) with a Fluorescent Spider-Like Receptor in Water

Abhishek Kumar Gupta,<sup>[a]</sup> Abhimanew Dhir,<sup>[a]</sup> and Chullikkattil P. Pradeep\*<sup>[a]</sup>

**Keywords:** Biosensors / Receptors / Fluorescence spectroscopy / Fluorescent probes / Anions

A series of water-soluble spider-like receptor molecules has been developed by the Schiff-base condensation of tris-(hydroxymethyl)aminomethane (TRIS) with various 2,6-diformylphenol (dfp) derivatives. The products were assessed for their anion sensing properties. Among these, the receptor

with a methoxy substituent showed selective fluorescent sensing towards adenosine-5'-triphosphate (ATP) and cytidine-5'-triphosphate (CTP) in contrasting modes in 100% aqueous media at pH 7.2.

## Introduction

The development of fluorescent chemosensors for nucleotides has received considerable attention in recent years due to the critical roles played by these anions in biological systems.<sup>[1]</sup> Among the various nucleotides, adenosine-5'-triphosphate (ATP) and cytidine-5'-triphosphate (CTP) are crucial for many fundamental activities of life.<sup>[2]</sup> ATP acts as universal energy source as well as extracellular signaling mediator for many biological processes.<sup>[3]</sup> Deficiency of ATP in the body can lead to hypoglycaemia, ischemia, and Parkinson's disease.<sup>[4]</sup> On the other hand, CTP plays important roles in the synthesis of nucleic acids, dolichol phosphorylation, and allosteric regulation of aspartate transcarbamylase.<sup>[5]</sup> In humans, CTP is involved in the transportation of cholesterol and fats, brain cell repair, and in the cure of nervous system related diseases.<sup>[6]</sup> Therefore, the detection and quantification of ATP and CTP in living cells under physiological conditions is highly important.<sup>[2,7]</sup> Nevertheless, the development of sensors for biological anions such as ATP or CTP is a challenging task compared with the development of sensors for metal ions or other smaller ions, because of the larger size of the former.<sup>[1c,8]</sup> Furthermore, such sensors need to function in aqueous media under physiological pH. Under biological conditions, hydrogen-bonding from water may compete and buffer any specific binding interaction between the host and the nucleotide guests, making the sensor design an even more challenging task.<sup>[9]</sup>

A variety of colorimetric and fluorescent probes have been reported for the detection of nucleotides in recent dec-

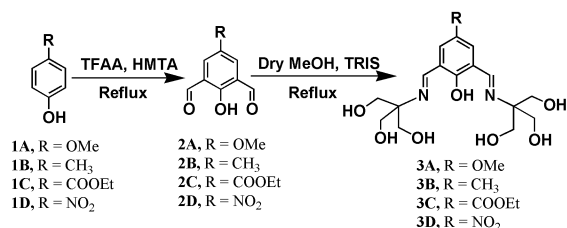
ades. These include chemosensors bearing imidazolium or quaternary ammonium groups as binding motifs, chemosensors based on hydrogen-bonding interactions containing azacrown, amide and urea moieties, chemosensors using zinc complexes or other metal complexes as the binding motifs, as well as chemosensors linked to polymers or mesoporous materials.<sup>[1]</sup> Some of the previously reported chemosensors for nucleotides contain aromatic groups as fluorescent moieties and hence require the use of a certain amount of nonaqueous solvents due to their limited solubility in water.<sup>[1i,1j]</sup>

Our research focuses on the development of new organic-inorganic hybrid materials for sensing applications.<sup>[10]</sup> In the present study, we have designed and developed a series of simple, 100% water soluble, spider-like Schiff-base receptor molecules, **3A–D**, starting from tris-(hydroxymethyl)aminomethane (TRIS) and 2,6-diformylphenol (dfp) derivatives, as shown in Scheme 1. Schiff bases of dfp derivatives have been widely explored in fluorescence sensing applications.<sup>[11]</sup> The attachment of two TRIS moieties with six  $-\text{CH}_2\text{OH}$  groups onto the dfp backbone could lead to water-soluble fluorescent receptors with large and flexible binding cavities.<sup>[12,13]</sup> These receptors are expected to undergo specific  $\text{O}-\text{H}\cdots\text{A}^-$  binding interactions with anions utilizing their  $-\text{CH}_2\text{OH}$ ,  $-\text{CH}=\text{N}-$ , and phenolic  $-\text{OH}$  groups.<sup>[14]</sup> Electron-donating and electron-withdrawing substituents have been introduced at the *para* position of the phenolic  $-\text{OH}$  group in these receptors to fine-tune their electronic and weak bonding properties. The evaluation of the fluorescence behavior of **3A–D** towards various anions in 100% aqueous media at pH 7.2 revealed that receptor **3A**, with electron-donating methoxy substituent, is capable of sensing ATP and CTP anions in contrasting modes. ATP generates a ratiometric fluorescence response, whereas CTP leads to simple fluorescence quenching behavior with **3A**. Ratiometric fluorescent probes have an important feature of permitting signal rationing, and

[a] School of Basic Sciences, Indian Institute of Technology Mandi, Mandi, Himachal Pradesh 175001, India  
E-mail: pradeep@iitmandi.ac.in  
<http://faculty.iitmandi.ac.in/~pradeep/>

Supporting information for this article is available on the WWW under <http://dx.doi.org/10.1002/ejoc.201403073>.

thus increase the dynamic range as well as provide built-in correction for environmental effects.<sup>[15]</sup> To our knowledge, a TRIS-scaffold-based receptor system for the selective detection of ATP and CTP in contrasting modes is unprecedented.



Scheme 1. Synthesis of TRIS-based spider-like receptor molecules; TFAA = Trifluoroacetic acid, HMTA = hexamethylenetetramine.

## Results and Discussion

### Synthesis of Receptors

Receptor molecules **3A**, **3C**, and **3D** were synthesized by Schiff-base condensation of the corresponding dfp derivatives<sup>[16]</sup> with TRIS in 1:2 molar ratio in methanol (Scheme 1); receptor **3B** was synthesized by following a reported procedure.<sup>[12]</sup> The formation of the TRIS-based Schiff bases, **3A–D**, was confirmed from their spectroscopic and analytical data. The IR spectra of receptors **3A**, **3C**, and **3D** each showed a characteristic C=N stretching band at 1639, 1633, and 1661  $\text{cm}^{-1}$ , respectively. No IR band corresponding to the free aldehyde group was observed, confirming 1:2 condensation in all cases. The  $^1\text{H}$  NMR spectra of **3A**, **3C**, and **3D** showed a singlet (12 H each) at  $\delta = 3.41$ , 3.43, and 3.55 ppm, respectively, corresponding to the  $\text{CH}_2$  protons of the TRIS moiety. Receptors **3A**, **3C**, and **3D** each exhibit an imino proton singlet corresponding to 2H at  $\delta = 9.94$ , 9.79, and 9.87 ppm, respectively. Full NMR spectra details are given in the Supporting Information. The formation of these receptors was further confirmed from their HRMS data, which showed parent ion peaks corresponding to the 1:2 condensation products at  $m/z$  387.1755 [**3A** + H]<sup>+</sup>, 429.1882 [**3C** + H]<sup>+</sup>, and 402.1593 [**3D** + H]<sup>+</sup> for receptors **3A**, **3C**, and **3D**, respectively (see the Supporting Information). The spectroscopic data therefore support the proposed structures of receptors **3A–D** (Scheme 1).

### Anion Binding Studies

The binding behavior of receptors **3A–D** towards 16 anions (ATP, ADP, AMP, CTP, PPI, F<sup>-</sup>, Cl<sup>-</sup>, Br<sup>-</sup>, I<sup>-</sup>, CH<sub>3</sub>COO<sup>-</sup>, CN<sup>-</sup>, SCN<sup>-</sup>, HSO<sub>4</sub><sup>-</sup>, H<sub>2</sub>PO<sub>4</sub><sup>-</sup>, ClO<sub>4</sub><sup>-</sup>, and NO<sub>3</sub><sup>-</sup>) was evaluated in TRIS buffer (pH 7.2) solution using fluorescence spectroscopic analyses. The spectra of compound **3A** in this 100% water medium showed fluorescence emission at 560 nm ( $5.0 \times 10^{-6}$  M,  $\lambda_{\text{ex}} = 457$  nm,  $\phi^{[17]} = 0.25$ ); details of the fluorescence studies are summarized in

Table 1 (see also the Supporting Information). Given that water was used as solvent (dielectric constant  $\epsilon = 80.2$  and dipole moment = 1.84 D), extensive H-bonding interactions of the receptor with solvent molecules was expected, which could provide rigidity to the system thus contributing to the observed fluorescence of compound **3A**.<sup>[11]</sup> In addition, the electron-donating nature of the methoxy group leads to intra-ligand ( $\pi$ - $\pi^*$ ) charge-transfer transition (ILCT) contributing to the observed emission of **3A**.<sup>[18,19]</sup> Among all the anions tested, compound **3A** showed a response only towards ATP and CTP ions in contrasting modes (see the Supporting Information). ATP (100 equiv.) generated a ratiometric fluorescence response with **3A**, whereas CTP (100 equiv.) showed simple fluorescence quenching behavior under identical experimental conditions (Figures 1 and 2). To check the role of buffer solutions on the sensing behavior, we also conducted similar experiments on **3A** in HEPES buffer (pH 7.2) and phosphate buffer (pH 7.2) solutions, but the results were quite similar to those obtained in TRIS

Table 1. Results of quantum yields, binding constants and detection limits of receptors **3A–D** with selected anions.

Receptors	$\phi$ [%]	Ali- quots	$K_b$ [ $\text{M}^{-1}$ ]	DL [M]
<b>3A</b>	0.25	ATP	$(7.61 \pm 0.01) \times 10^3$ (Figure 5)	$3.9 \times 10^{-6}$ (Figure 7)
		CTP	$(1.19 \pm 0.03) \times 10^4$ (Figure 6)	$8.3 \times 10^{-6}$ (Figure 8)
<b>3B</b>	0.32	–	–	–
<b>3C</b>	0.36	–	–	–
<b>3D</b> <sup>[a]</sup>	0.006 <sup>[b]</sup>	ATP	$(2.98 \pm 0.003) \times 10^2$	$5.0 \times 10^{-5}$

[a] Binding isotherm and detection limit curve for receptor **3D** are given in the Supporting Information. [b]  $\phi^{\text{s}} = 0.035$ , is the quantum yield of **3D** after addition of ATP.

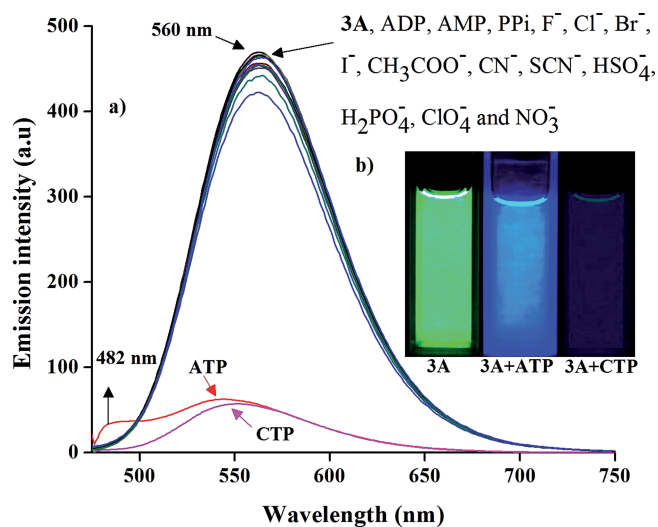


Figure 1. (a) Luminescence response of **3A** ( $5.0 \times 10^{-6}$  M) upon addition of various anions (ATP, ADP, AMP, CTP, PPI, F<sup>-</sup>, Cl<sup>-</sup>, Br<sup>-</sup>, I<sup>-</sup>, CH<sub>3</sub>COO<sup>-</sup>, CN<sup>-</sup>, SCN<sup>-</sup>, HSO<sub>4</sub><sup>-</sup>, H<sub>2</sub>PO<sub>4</sub><sup>-</sup>, ClO<sub>4</sub><sup>-</sup> and NO<sub>3</sub><sup>-</sup>; 100.0 equiv., 0.5 mM) in 0.05 M TRIS buffer (pH 7.2);  $\lambda_{\text{ex}} = 457$  nm.

buffer solution, dismissing any influential role of buffer on the sensing behavior of the receptor (see the Supporting Information).

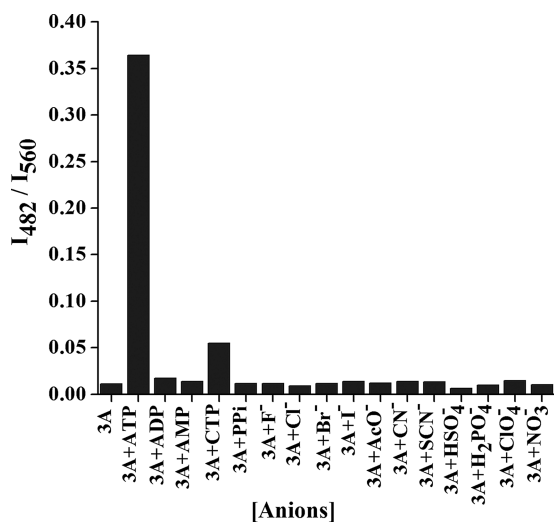


Figure 2. Ratiometric ( $I_{482}/I_{560}$ ) selectivity of **3A** ( $5.0 \times 10^{-6}$  M) upon addition of different anions in TRIS buffer (pH 7.2).

To gain insight into the mechanism of fluorescence changes occurring upon addition of ATP and CTP to **3A**,  $^1\text{H}$  and  $^{31}\text{P}$  NMR spectroscopic studies were conducted on solutions of **3A** by adding equimolar solutions of ATP and CTP (Figures 3 and 4) separately. When ATP was added to a solution of **3A**, the two aromatic protons ( $\text{H}_2$  and  $\text{H}_8$ , see Figure 3, a) of the adenine unit of ATP showed upfield shifts from 8.21 and 8.41 ppm to 8.05 and 8.36 ppm, respec-

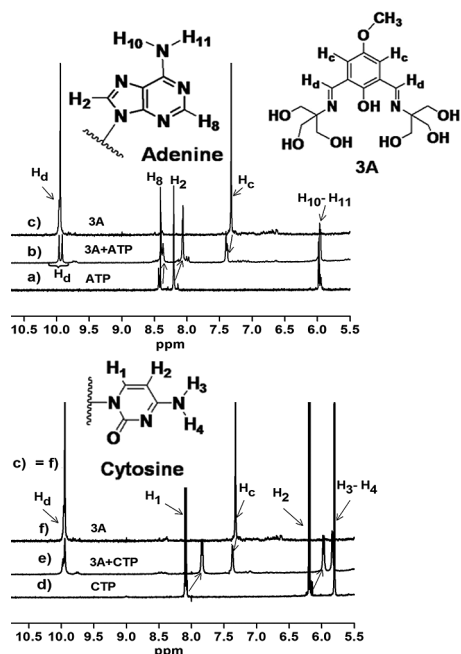


Figure 3. (a) Partial  $^1\text{H}$  NMR spectra (aromatic region) of ATP ( $10^{-2}$  M). (b) ATP in the presence of **3A** (1:1 molar ratio). (c) **3A** (aromatic region). (d) Partial  $^1\text{H}$  NMR spectra (aromatic region) of CTP ( $10^{-2}$  M). (e) CTP in the presence of **3A** (1:1 molar ratio). (f) **3A** (aromatic region) taken in  $\text{D}_2\text{O}$ .

tively ( $\Delta\delta = 0.16$  and  $0.05$  ppm, respectively) (Figure 3, b). In addition, the  $\text{H}_c$  (Figure 3, c) protons of receptor **3A** showed downfield shift from 7.32 to 7.40 ppm ( $\Delta\delta = 0.08$  ppm) and the signal due to imino protons  $\text{H}_d$  (Figure 3, b) showed splitting, indicating that the imino protons exist in different chemical environments in presence of ATP (also see the Supporting Information).  $^{31}\text{P}$  NMR spectrum of **3A** in  $\text{D}_2\text{O}$  in the presence of added ATP (Figure 4, e) showed large downfield shifts of the  $\gamma$ - and  $\beta$ -phosphorus signals of ATP ( $\Delta\delta = 2.41$  and  $0.56$  ppm, respectively) (Figure 4, e).

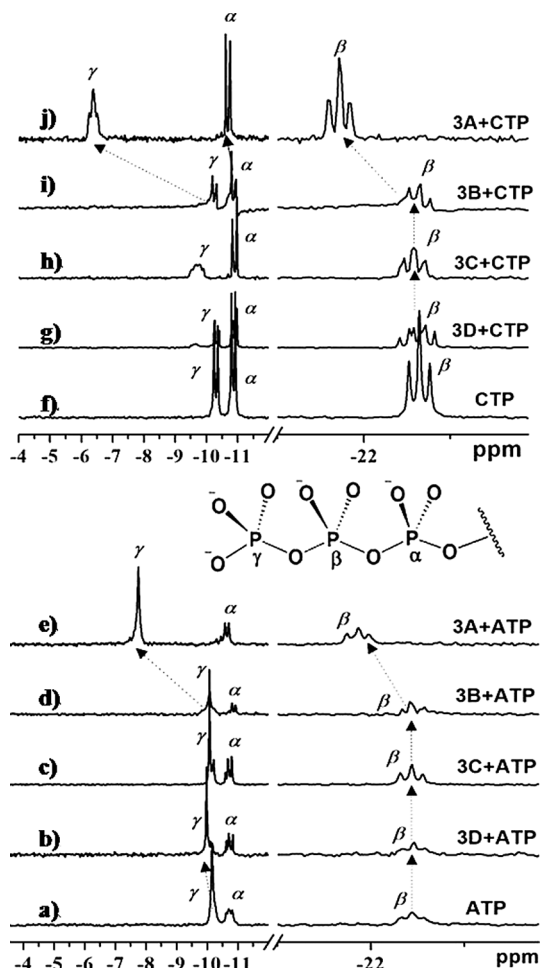


Figure 4. (a)  $^{31}\text{P}$  NMR spectra (in  $\text{D}_2\text{O}$ ) of pure ATP ( $10^{-2}$  M). (b) ATP in presence of **3D** (1 equiv.). (c) ATP in presence of **3C** (1 equiv.). (d) ATP in presence of **3B** (1 equiv.). (e) ATP in presence of **3A** (1 equiv.). (f)  $^{31}\text{P}$  NMR of CTP ( $10^{-2}$  M). (g) CTP in presence of **3D** (1 equiv.). (h) CTP in presence of **3C** (1 equiv.). (i) CTP in presence of **3B** (1 equiv.). (j) CTP in presence of **3A** (1 equiv.).

We performed similar NMR studies on **3A** through the addition of equimolar amounts of CTP and observed that the original peak positions of cytosine protons  $\text{H}_1$  and  $\text{H}_2$  (Figure 3, d) showed upfield shifts from 8.08 and 6.19 ppm to 7.83 and 5.95 ppm, respectively ( $\Delta\delta = 0.25$  and  $0.24$  ppm, see Figure 3, e). The receptor protons  $\text{H}_c$  showed a downfield shift from 7.32 to 7.38 ppm ( $\Delta\delta = 0.06$  ppm, see Figure 3, e) (see the Supporting Information). One im-

portant observation here is that the imino protons,  $H_d$ , did not show any peak splitting, unlike the coupling observed in the case of ATP addition, indicating that the imino protons of **3A** exist in a similar chemical environment in the presence of CTP.  $^{31}\text{P}$  NMR spectra of CTP (Figure 4, j) showed downfield shifts in peak position of  $\gamma$ -,  $\beta$ -, and  $\alpha$ -phosphorus centers ( $\Delta\delta = 3.93$ ,  $0.93$ , and  $0.18$  ppm, respectively) in equimolar solutions with **3A** (Figure 4, j), which are higher than those observed in the case of ATP.  $^{31}\text{P}$  NMR studies conducted by using different concentrations of the receptor and analytes resulted in similar peak shifts, suggesting that the concentrations of the receptor and analytes do not affect the sensing mechanism considerably (see the Supporting Information).

The above NMR studies clearly demonstrated complexation induced shifts (CISs) of certain important protons of the receptor as well as the guests, suggesting the existence of some binding interactions between receptor **3A** and the guests ATP and CTP in solutions.<sup>[1j,20]</sup> The formation of 1:1 complexes **3A**·ATP and **3A**·CTP were further confirmed by HRMS analyses. Parent ion peaks at  $954.8256$  and  $909.9168$  corresponding to the species  $[\mathbf{3A}+(\text{ATP}-\text{Na}+\text{K})+\text{H}]^+$  and  $[\mathbf{3A}+(\text{CTP}-\text{Na}+\text{H})+\text{H}_2\text{O}+\text{H}]^+$  (ATP and CTP used were disodium salts) were observed in the mass spectra of equimolar solutions of **3A**·ATP and **3A**·CTP, respectively (see the Supporting Information). The binding constants ( $K_b$ )<sup>[14c,21]</sup> for the formation of hydrogen bonded complexes **3A**·ATP and **3A**·CTP were calculated as  $(7.61 \pm 0.01) \times 10^3 \text{ M}^{-1}$  and  $(1.19 \pm 0.03) \times 10^4 \text{ M}^{-1}$ , respectively, and are summarized in Table 1 (Figures 5 and 6). The Job's plot<sup>[22]</sup> of **3A** with ATP and CTP showed the formation of 1:1 complexes between receptor **3A** and the analytes (ATP and CTP) (see the Supporting Information). The detection limits<sup>[23]</sup> of **3A** as a fluorescence sensor for the analysis of ATP and CTP were determined from plots of fluorescence intensity versus the concentration of added ATP and CTP. Detection limits (DL) of **3A** towards ATP

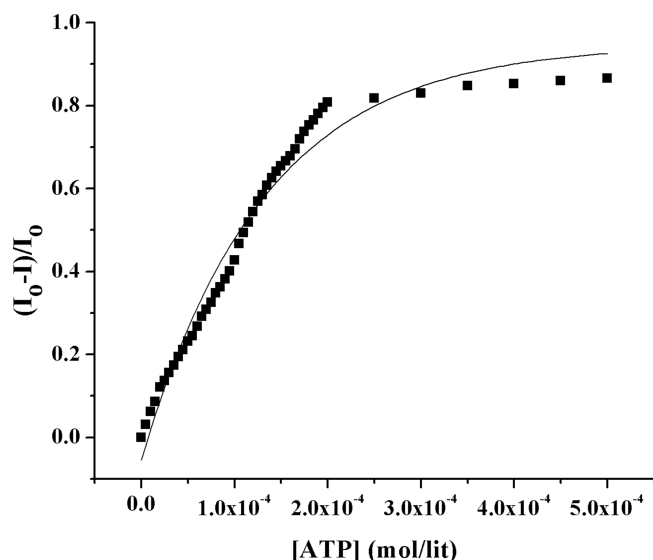


Figure 5. Binding isotherm of **3A** after addition of ATP.

and CTP were found to be  $3.9 \times 10^{-6}$  and  $8.3 \times 10^{-6}$  M, respectively, see Table 1, (Figure 7 and Figure 8), which are comparable to those of similar systems.<sup>[24]</sup>

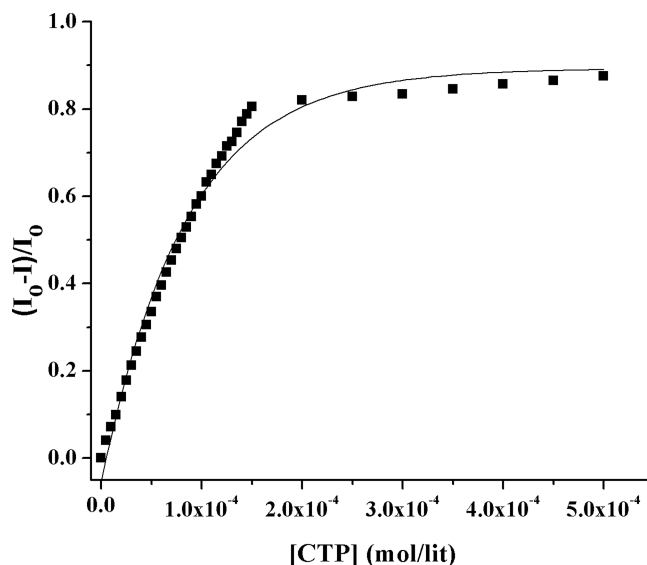


Figure 6. Binding isotherm of **3A** after addition of CTP.

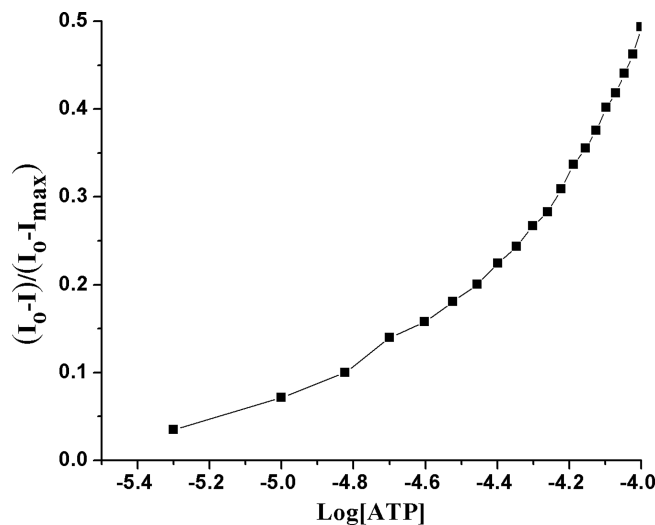


Figure 7. A plot of  $(I_0 - I)/(I_0 - I_{\text{max}})$  vs.  $\log[\text{ATP}]$  for **3A** in presence of the ATP.

Based on the above analytical and spectroscopic data, the following observations can be made. The differences observed in the NMR peak shifts of ATP and CTP protons reveal that their mode and extent of binding with **3A** are different. Especially, there are pronounced variations in the shifts of imino protons of the receptor as well as the phosphorus peaks of the guests, suggesting different modes of binding of these guests with **3A**. This was further confirmed by binding constant measurements, which suggest that receptor **3A** exhibits better binding properties with CTP in comparison to ATP. Therefore, based on the fluorescence,  $^1\text{H}$  NMR,  $^{31}\text{P}$  NMR, HRMS, and binding constant analyses results, we propose the possible binding modes of receptor **3A** with ATP and CTP as shown in Figure 9. As per

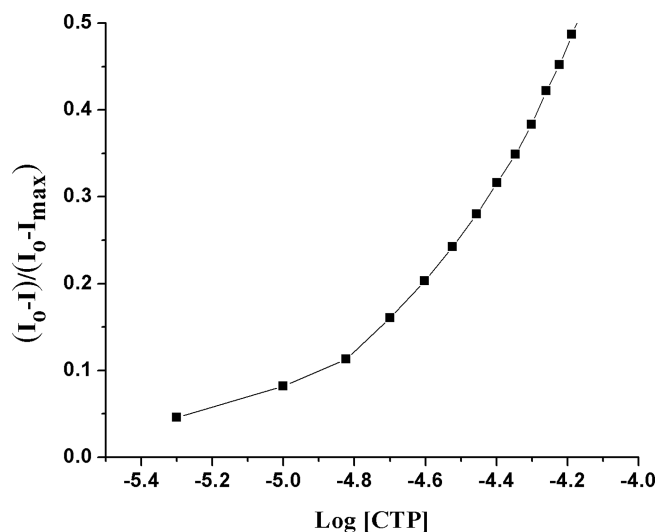


Figure 8. A plot of  $(I_0 - I)/(I_0 - I_{max})$  vs.  $\log[CTP]$  for **3A** in presence of the CTP.

this, **3A** binds to ATP through H-bond interactions using its phenolic –OH as well as the –CH<sub>2</sub>OH group on one of its TRIS arms. The second TRIS arm remains free in this proposed model, facilitating ILCT through this arm<sup>[25,26]</sup> in **3A**·ATP complex (Figure 9, a) leading to blueshifted fluorescence emission and ultimately to ratiometric fluorescence response on subsequent additions of ATP.

With CTP, **3A** uses –CH<sub>2</sub>OH groups from both of its TRIS arms (Figure 9, b) in addition to the phenolic –OH group, resulting in strong binding, as revealed by NMR as well as binding constant calculation studies. This mechanism is also in accordance with the NMR results, whereby the peak due to the imino protons of the receptor shows splitting in the presence of ATP but not in the presence of CTP. The involvement of both the arms of **3A** in the formation of hydrogen-bonded complex inhibits the ILCT phenomenon, resulting in quenching of fluorescence. The NMR peak shifts observed for the aromatic proton H<sub>c</sub> of the receptor as well as the adenine/cytosine protons of the guests suggest weak  $\pi$ – $\pi$  stacking interaction between these units, as shown in Figure 9. These weak interactions are expected to play significant roles in the overall binding pro-

cess as well as in the observed fluorescence intensity reduction of receptor **3A** in the presence of ATP and CTP.<sup>[14b,27]</sup> Control experiments performed on **3A** using sodium triphosphate as analyte did not show any sensing (see the Supporting Information), reiterating the role of these aromatic  $\pi$ – $\pi$  stacking interactions in the sensing mechanism. Any mediating role of sodium metal in the binding process has also been ruled out by studying the fluorescence properties of **3A** in the presence of sodium salts such as sodium triphosphate and sodium perchlorate, which did not show any quenching (see the Supporting Information). Proposed model of the complexes **3A**·ATP and **3A**·CTP were supported by optimized structures (see the Supporting Information).

Under similar experimental conditions, we also evaluated the sensing behavior of receptors **3B–D** towards various anions (ATP, ADP, AMP, CTP and PPi). Receptors **3B** and **3C** are found to exhibit significant fluorescence emission ( $\lambda_{ex}$  = 430 and 403 nm,  $\phi^{[21]}$  = 0.32 and 0.36, respectively; Table S1) in water solutions. No significant changes in their emission behavior was observed upon addition of anions under the experimental conditions (see the Supporting Information). These results are also supported by NMR studies; for example, no significant shift in peak positions of ATP was observed in the presence of **3B** and **3C** [Figure 4 (c and d)]. Conversely, receptor **3D** did not exhibit any significant fluorescence emission ( $\lambda_{ex}$  = 385 nm,  $\phi^{[17]}$  = 0.006) (Table 1, also see the Supporting Information) in water solutions, which can be ascribed to the PET<sup>[28]</sup> effect operating due to the presence of a strong electron-withdrawing –NO<sub>2</sub> group on its structural backbone.<sup>[29]</sup> On addition of an equimolar amount of ATP solution, receptor **3D** showed enhancement in its fluorescence intensity ( $\phi^{[17]}$  = 0.032), which may be attributed to the negation of PET effects on binding with ATP molecule. The <sup>31</sup>P NMR spectrum of ATP in the presence of **3D** showed a small shift in the peak position of  $\gamma$ -phosphorus compared with that of **3B** and **3C**, suggesting the existence of some binding interaction between **3D** and ATP (Figure 4, b). This comparison of behavior of **3A** with **3B–D** indicates that the ratiometric sensing of ATP in **3A** is regulated by the electron-donating nature of the methoxy group present in **3A**.

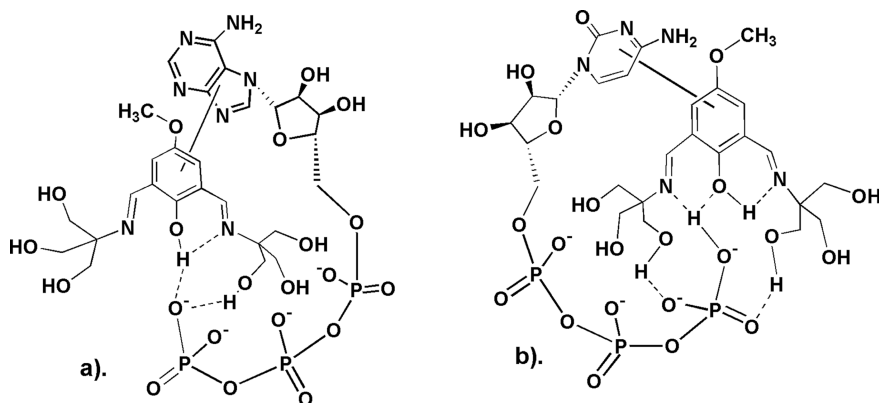


Figure 9. Proposed binding mode of **3A** with (a) ATP and (b) CTP.

We also carried out transmission electron microscopic (TEM) studies on mixtures of ATP and CTP with **3A** (Figure 10). TEM analysis revealed some aggregation behavior of **3A** following complex formation with ATP/CTP. Perhaps this aggregation of complex units, due to various weak bonding interactions, may lead to the generation of some kind of hydrophobic microenvironment around the complex units, thus preventing further interference from solvent water molecules. A distinct morphology difference was also observed in the existing morphology of **3A** on addition of ATP and CTP, confirming that the analytes interact with **3A** in different modes.

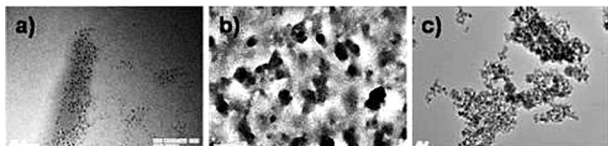


Figure 10. (a) Typical TEM image of receptor **3A** ( $5.0 \times 10^{-4}$  M). (b) **3A** in presence of ATP (1.0 equiv.). (c) **3A** in presence of CTP (1.0 equiv.) in water. Scale bar 100 nm in all cases.

The above studies clearly show the exceptional binding behavior of **3A** with ATP and CTP in aqueous solutions compared with other members of the receptor series. Therefore, we were interested to study the solid-state<sup>[10d]</sup> fluorescence behavior of **3A** with ATP and CTP as well. To this end, a solution of **3A** ( $5.0 \times 10^{-4}$  M) in TRIS buffer (0.05 M, pH 7.2) was adsorbed on TLC plate. This spot showed strong emissions under UV irradiation (254 and 365 nm) but became nonemissive when a drop of ATP or CTP solution (1.0 equiv.) was adsorbed over it (Figure 11). This experiment clearly shows that the receptor **3A** also exhibits binding behavior with ATP and CTP in the solid state, as observed earlier in the solution state.

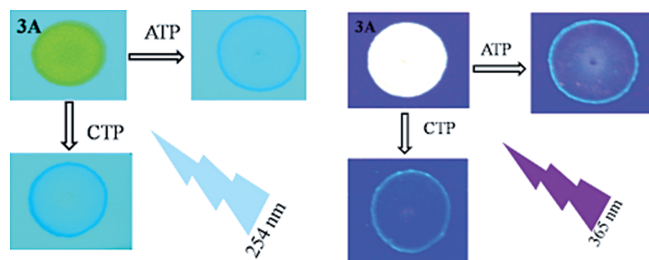


Figure 11. Solid-state detection (under illumination at 254 and 365 nm UV light) on silica gel coated TLC plate. Spots of receptor **3A** in the absence and in the presence of ATP and CTP.

## Conclusions

We have designed a series of simple, 100% water soluble receptor molecules **3A–D**, having multiple weak-bonding sites and different electron-donating/-withdrawing groups on the structural backbone. Of these receptors, compound **3A**, with a methoxy substituent, acts as a fluorescence chemosensor for the detection of ATP and CTP in micromolar concentrations in 100% water solutions with unique

recognition and sensing properties. With ATP, this receptor showed ratiometric fluorescence behavior, but with CTP it exhibited simple fluorescence quenching. Naked eye detection of ATP/CTP in the solid state was also possible with this receptor.

## Experimental Section

**General:** All reagents were purchased from Sigma–Aldrich and were used without further purification. TRIS buffer (pH 7.2) was used to perform analytical studies. All the fluorescence spectra were recorded with an Agilent Technologies Cary Eclipse fluorescence spectrophotometer. UV/Vis spectra were recorded with a Shimadzu UV-2450 spectrophotometer and FTIR spectra were recorded with a PerkinElmer FTIR spectrometer (Spectrum Two, Serial No:88689). ESI-TOF HRMS spectra were recorded with a Bruker maxis impact instrument.  $^1\text{H}$  and  $^{13}\text{C}$  NMR spectra were recorded with a Joel JNM ECS-400 FT-NMR spectrometer using  $\text{D}_2\text{O}$  as solvent and TMS as internal standard. Data are reported as follows: chemical shift in ppm ( $\delta$ ), multiplicity (s = singlet, d = doublet, br = broad singlet, m = multiplet), coupling constant  $J$  (Hz). Solutions of compounds **3A–D**, sodium salts of adenosine triphosphate (ATP), adenosine diphosphate (ADP), adenosine monophosphate (PPi), and tetrabutyl ammonium salts of anions ( $\text{F}^-$ ,  $\text{Cl}^-$ ,  $\text{Br}^-$ ,  $\text{I}^-$ ,  $\text{CH}_3\text{COO}^-$ ,  $\text{CN}^-$ ,  $\text{SCN}^-$ ,  $\text{HSO}_4^-$ ,  $\text{H}_2\text{PO}_4^-$ ,  $\text{ClO}_4^-$  and  $\text{NO}_3^-$ ) were prepared in 0.05M TRIS buffer (pH 7.2).<sup>[30]</sup>

**General Procedure for the Preparation of Compounds 2A–D:** Compound **2A**,<sup>[16a]</sup> **2B**,<sup>[16b]</sup> **2C**,<sup>[16c]</sup> and **2D**<sup>[16d]</sup> were synthesized by Duff reaction using reported procedures.

**General Procedure for the Preparation of Compounds 3A–D:** Dissolved 2,6-diformylphenol (dfp) derivatives **2A–D** (4.5 mmol) in anhydrous MeOH (15 mL) were heated for 15 min at 70 °C. When a clear yellow solution of **2A–D** was obtained, tris(hydroxymethyl)aminomethane (TRIS) (9 mmol, 1.09 g) was added and the resulting solution was heated to reflux for 6 h under a nitrogen atmosphere to give an orange gummy product on solvent evaporation. The product was washed sequentially with chloroform and diethyl ether and dried under vacuum to give the product **3A–D**.

**Compound 3A:** Yield 1.38 g (80%); orange solid; m.p.  $255 \pm 5$  °C. IR (KBr):  $\tilde{\nu} = 3428$  (O–H), 2938 (C–H), 1543 (OCH<sub>3</sub>), 1639 (C=N)  $\text{cm}^{-1}$ .  $^1\text{H}$  NMR (400 MHz,  $\text{D}_2\text{O}$ ):  $\delta = 9.94$  (s, 2 H, HC=N), 7.32 (s, 2 H, Ar-H), 3.72 (s, 3 H, CH<sub>3</sub>), 3.41 (s, 12 H, CH<sub>2</sub>) ppm.  $^{13}\text{C}$  NMR (100 MHz,  $\text{D}_2\text{O}$ ):  $\delta = 193.5$ , 165.9, 147.0, 128.1, 122.8, 61.91, 60.4, 57.8 ppm. HRMS:  $m/z$  calcd. for  $\text{C}_{17}\text{H}_{26}\text{N}_2\text{O}_8$  [ $\text{M} + \text{H}$ ]<sup>+</sup> 387.1767; found 387.1755 (see the Supporting Information).

**Compound 3B:** Synthesized by using a reported procedure.<sup>[12]</sup>

**Compound 3C:** Yield 1.70 g (88.2%); yellow solid; m.p. 114 °C. IR (KBr):  $\tilde{\nu} = 3344$  (O–H), 2938 (C–H), 1681 (C=O, ester), 1633 (C=N)  $\text{cm}^{-1}$ .  $^1\text{H}$  NMR (400 MHz,  $\text{D}_2\text{O}$ ):  $\delta = 9.79$  (s, 2 H, HC=N), 7.98 (s, 2 H, Ar-H), 4.08 (q,  $J = 8.0$  Hz, 2 H, CH<sub>2</sub>), 3.43 (s, 12 H, CH<sub>2</sub>), 1.14 (t,  $J = 8.0$  Hz, 3 H, CH<sub>3</sub>) ppm.  $^{13}\text{C}$  NMR (100 MHz,  $\text{D}_2\text{O}$ ):  $\delta = 193.4$ , 167.8, 166.5, 138.9, 127.7, 112.6, 61.7, 60.2, 58.0, 13.4 ppm. HRMS:  $m/z$  calcd. for  $\text{C}_{19}\text{H}_{29}\text{N}_2\text{O}_9$  [ $\text{M} + \text{H}$ ]<sup>+</sup> 429.1873; found 429.1880 (see the Supporting Information).

**Compound 3D:** Yield 1.26 g (70%); yellow solid; m.p. 260 °C. IR (KBr):  $\tilde{\nu} = 3310$  (O–H), 2928 (C–H), 1560 (NO<sub>2</sub>), 1661 (C=N)  $\text{cm}^{-1}$ .  $^1\text{H}$  NMR (400 MHz,  $\text{D}_2\text{O}$ ):  $\delta = 9.87$  (s, 2 H, HC=N), 8.34 (s, 2 H, Ar-H), 3.55 (s, 12 H, CH<sub>2</sub>) ppm.  $^{13}\text{C}$  NMR (100 MHz,  $\text{D}_2\text{O}$ ):  $\delta = 193.3$ , 179.9, 133.5, 133.0, 127.7, 61.1, 58.9 ppm. HRMS:

$m/z$  calcd. for  $C_{16}H_{24}N_3O_9$   $[M + H]^+$  402.1512; found 402.1590 (see the Supporting Information).

**UV/Vis and Fluorometric Analysis:** All UV/Vis and spectrofluorometric titrations were performed on 5  $\mu$ M solutions of the receptors at pH 7.2 in 0.05 M TRIS buffer/water mixture. Freshly prepared standard solutions ( $10^{-1}$  to  $10^{-3}$  M) of ATP, ADP, AMP, CTP, PPI,  $F^-$ ,  $Cl^-$ ,  $Br^-$ ,  $I^-$ ,  $CH_3COO^-$ ,  $CN^-$ ,  $SCN^-$ ,  $HSO_4^-$ ,  $H_2PO_4^-$ ,  $ClO_4^-$ , and  $NO_3^-$  (as the corresponding sodium and tetrabutyl ammonium salts) in pH 7.2, 0.05 M TRIS buffer/water mixture were used to record the UV/Vis and fluorescence spectra. Solutions of the receptors **3A–D** (3 mL) were taken in a quartz cuvette (path length 1 cm) and solutions of anions were added to these solutions by using micropipette.

**Determination of Detection Limit:** Fluorescence titration experiments on **3A** with ATP and CTP and on **3D** with ATP were carried out by adding aliquots of ATP and CTP solutions of micromolar concentrations to receptor solutions and the curve between  $[(I_0 - I)/(I_0 - I_{max})]$  vs.  $\log[Anion]$  was plotted ( $I_0$  is initial intensity,  $I_{max}$  is final intensity and  $I$  is change in intensity after each addition of anions). A linear regression curve was fitted to anion concentration. The point at which this line crossed the ordinate axis was taken as the detection limit.<sup>[23]</sup>

**Determination of Quantum Yields:** The fluorescence quantum yields of receptors **3A–D** were determined at room temperature in TRIS buffer (pH 7.2) by using optically matching solutions. Quinine sulfate ( $\phi_f = 0.53$  in 0.05 M  $H_2SO_4$ ) was used as the standard at an excitation wavelength of 347 nm for these measurements. The quantum yield was calculated by using the Equation (1).<sup>[17]</sup>

$$\phi_s = \phi_r \times \frac{\eta_s^2}{\eta_r^2} \times \frac{I_s}{A_s} \times \frac{A_r}{I_r} \quad (1)$$

where  $\phi_s$  is the radiative quantum yield of the sample,  $\phi_r$  is the radiative quantum yield of reference,  $A_s$  and  $A_r$  are the absorbances of the sample and the reference, respectively,  $I_s$  and  $I_r$  are the integrated areas of emission for the sample and reference, respectively, and  $\eta_s$  and  $\eta_r$  are the refractive index of the sample and the reference solutions, respectively (pure solvents were assumed).

**Binding Constants:** The fluorimetric titrations on **3A** were performed at 25 °C in TRIS buffer (pH 7.2) measuring the quenching of the emission at 560 nm. Binding constant  $K_b$  for the anions were calculated from the plots of  $[(I_0 - I)/I_0]$  vs.  $[anion]$  by using nonlinear curve fitting using Origin lab 8.0.<sup>[14c,21,31]</sup>

**Supporting Information** (see footnote on the first page of this article): NMR, mass, UV/Vis, and fluorescence spectra and fluorescence titration data, tables Job's plot and optimized structures.

## Acknowledgments

C. P. P. thanks the Department of Science and Technology (DST), New Delhi for funds under the fast track Scheme Grant SR/FT/CS-58/2011 and IIT Mandi for infrastructural facilities as well as financial support through a Seed Grant. A. K. G. thanks the Ministry of Human Resource Development (MHRD), Govt. of India for a fellowship. Helpful suggestions from Mr. Ashish Bahuguna related to some experimental procedures is acknowledged.

[1] a) E. García-España, R. Belda, J. González, J. Pitarch, A. Bianchi, in: *Supramolecular Chemistry: From Molecules to Nano-*

- materials* (Eds.: P. A. Gale, J. W. Steed), John Wiley & Sons, Ltd. **2012**, p. 1225–1257; b) Y. Zhou, Z. Xu, J. Yoon, *Chem. Soc. Rev.* **2011**, *40*, 2222–2235; c) R. Martínez-Mañez, F. Sanconón, *Chem. Rev.* **2003**, *103*, 4419–4476; d) Z. Xu, S. K. Kim, J. Yoon, *Chem. Soc. Rev.* **2010**, *39*, 1457–1466; e) P. A. Gale, *Chem. Soc. Rev.* **2010**, *39*, 3746–3771; f) S. K. Kim, J. L. Sessler, *Chem. Soc. Rev.* **2010**, *39*, 3784–3809; g) A.-F. Li, J.-H. Wang, F. Wang, Y.-B. Jiang, *Chem. Soc. Rev.* **2010**, *39*, 3729–3745; h) Z. Xu, X. Chen, H. N. Kim, J. Yoon, *Chem. Soc. Rev.* **2010**, *39*, 127–137; i) Z. Kejik, K. Záruba, D. Michalík, J. Šebek, J. Dain, S. Pataridis, K. Volka, V. Král, *Chem. Commun.* **2006**, 1533–1535; j) H. Wang, W. H. Chan, *Org. Biomol. Chem.* **2008**, *6*, 162–168.
- [2] a) For enzyme-catalyzed phosphoryl transfer reactions, see: J. R. Knowles, *Annu. Rev. Biochem.* **1980**, *49*, 877–919; b) A. K. H. Hirsch, F. R. Fischer, F. Diederich, *Angew. Chem. Int. Ed.* **2007**, *46*, 338–352; *Angew. Chem.* **2007**, *119*, 342; c) D. H. Lee, J. H. Im, S. U. Son, Y. K. Chung, J.-I. Hong, *J. Am. Chem. Soc.* **2003**, *125*, 7752–7753.
- [3] a) S. V. Khlyntseva, Y. R. Bazel, A. B. Vishnikina, V. Andrich, *J. Anal. Chem.* **2009**, *64*, 657–673; b) P. Ritter, *Biochemistry a Foundation*; Creation Research Society Quarterly June **1999**, Brooks/Cole, Pacific Grove, CA, **1996**, 36.
- [4] P. Mahato, A. Ghosh, S. K. Mishra, A. Shrivastav, S. Mishra, A. Das, *Chem. Commun.* **2010**, *46*, 9134–9136.
- [5] J. C. M. Allen, J. R. Kalin, J. Sack, D. Verizzo, *Biochemistry* **1978**, *17*, 5020–5026.
- [6] O. Tollbom, G. Dallner, *Br. J. Exp. Path.* **1986**, *67*, 757–764.
- [7] D. Mallikarachchi, D. S. Burz, N. M. Allewell, *Biochemistry* **1989**, *28*, 5386–5391.
- [8] P. D. Beer, P. A. Gale, *Angew. Chem. Int. Ed.* **2001**, *40*, 486–516; *Angew. Chem.* **2001**, *113*, 502.
- [9] H. Ahmad, B. W. Hazel, A. J. H. M. Meijer, J. A. Thomas, K. A. Wilkinson, *Chem. Eur. J.* **2013**, *19*, 5081–5087.
- [10] a) M. Devi, A. Dhir, Pooja, C. P. Pradeep, *RSC Adv.* **2014**, *4*, 27098–27105; b) M. Devi, A. Dhir, C. P. Pradeep, *Dalton Trans.* **2013**, *42*, 7514–7518; c) A. K. Gupta, A. Dhir, C. P. Pradeep, *Dalton Trans.* **2013**, *42*, 12819–12823; d) S. Sharma, A. Dhir, C. P. Pradeep, *Sens. Actuators, B* **2014**, *191*, 445–449; e) D. Rambabu, Pooja, C. P. Pradeep, A. Dhir, *J. Mater. Chem. A* **2014**, *2*, 8628–8631; f) D. Rambabu, C. P. Pradeep, A. Dhir, *Inorg. Chem. Front.* **2014**, *1*, 163–166.
- [11] M. Mukhopadhyay, D. Banerjee, S. Mukherjee, *J. Phys. Chem. A* **2006**, *110*, 12743–12751.
- [12] V. Chandrasekhar, S. Das, R. Yadav, S. Hossain, R. Parihar, G. Subramaniam, P. Sen, *Inorg. Chem.* **2012**, *51*, 8664–8666.
- [13] T. Yang, W. Qin, W. Liu, *Talanta* **2004**, *62*, 451–456.
- [14] a) S. Sen, M. Mukherjee, K. Chakrabarty, I. Hauli, S. K. Mukhopadhyay, P. Chattopadhyay, *Org. Biomol. Chem.* **2013**, *11*, 1537–1544; b) A. Dorazco-González, M. F. Alamo, C. Godoy-Alcántar, H. Hpf, A. K. Yatsimirsky, *RSC Adv.* **2014**, *4*, 455–466; c) M. Yousuf, N. Ahmed, B. Shirinfar, V. M. Miriyala, S. Youn, K. S. Kim, *Org. Lett.* **2014**, *16*, 2150–2153.
- [15] A. Dhir, V. Bhalla, M. Kumar, *Tetrahedron Lett.* **2008**, *49*, 4227–4230.
- [16] a) H. Sharghi, M. N. Ali, K. Niknam, *J. Org. Chem.* **2001**, *66*, 7287–7293; b) D. K. Paul, J. P. W. Andrew, K. C. Williams, *Inorg. Chem.* **2008**, *47*, 11711–11719; c) N. K. Lifshin, L. Albertazzi, M. Bendikov, P. S. Baran, D. Shabat, *J. Am. Chem. Soc.* **2012**, *134*, 20412–20420; d) A. Hryniewicka, A. Kozłowska, S. Witkowski, *J. Organomet. Chem.* **2012**, *701*, 87–92.
- [17] A. M. Brouwer, *Pure Appl. Chem.* **2011**, *83*, 2213–2228.
- [18] C. B. Larsen, H. V. Salm, C. A. Clark, A. B. S. Elliott, M. G. Fraser, R. Horvath, N. T. Lucas, X. Z. Sun, M. W. George, K. C. Gordon, *Inorg. Chem.* **2014**, *53*, 1339–1354.
- [19] a) J. R. Lakowicz, *Topics in Fluorescence Spectroscopy: Probe Design and Chemical Sensing*; Plenum Press, New York, **1994**, 4; b) J. P. Desvergne, A. W. Czarnik, *Chemosensors of Ion and Molecule Recognition*, NATO ASI Series, Kluwer Academic Publishers, Dordrecht, The Netherlands, **1997**.

- [20] C. Bazzicalupi, S. Biagini, A. Bencini, E. Faggi, C. Giorgi, I. Matera, B. Valtancoli, *Chem. Commun.* **2006**, 39, 4087–4089.
- [21] a) K. A. Connors, *Binding Constants: The Measurement of Molecular Complex Stability*, John Wiley & Sons, New York, **1987**, p. 50–65; b) E. Cielen, A. Tahri, K. V. Heyen, G. J. Hoonart, F. C. De Schryver, N. J. Boens, *J. Chem. Soc. Perkin Trans. 2* **1998**, 1573–1580.
- [22] J. C. Canzoneri, A. K. Oyelere, *Nucleic Acids Res.* **2008**, 36, 6825–6834.
- [23] M. Shortreed, R. Kopelman, M. Kuhn, B. Hoyland, *Anal. Chem.* **1996**, 68, 1414–1418.
- [24] a) X. Liu, J. Xu, Y. Lv, W. Wu, W. Liu, Y. Tang, *Dalton Trans.* **2013**, 42, 9840–9846; b) X. J. Zhao, R. X. He, Y. F. Li, *Analyst* **2012**, 137, 5190–5192.
- [25] S. Sinha, T. Mukherjee, J. Mathew, S. K. Mukhopadhyay, S. Ghosh, *J. Photochem. Photobiol. A: Chem.* **2014**, 277, 75–81.
- [26] a) M. Prabhakar, P. S. Zacharias, S. K. Das, *Inorg. Chem.* **2005**, 44, 2585–2587; b) A. Sarkar, A. K. Ghosh, V. Bertolasi, D. Ray, *Dalton Trans.* **2012**, 41, 1889–1896.
- [27] a) G. Zong, L. Xian, G. Lu, *Tetrahedron Lett.* **2007**, 48, 3891–3894; b) P. P. Neelakandan, M. Hariharan, D. Ramaiah, *Org. Lett.* **2005**, 7, 5765–5768.
- [28] B. Valeur, I. Leray, *Coord. Chem. Rev.* **2000**, 205, 3–40.
- [29] C. P. Pradeep, *Acta Crystallogr., Sect. E: Struct. Biol. Cryst. Commun.* **2005**, 61, o3825–o3827.
- [30] D. D. Perrin, B. Dempsey, *Buffers for pH and Metal Ion Control*, John Wiley & Sons, New York, **1974**.
- [31] T. Mistri, R. Alam, M. Dolai, S. K. Mandal, P. Guha, A. R. K. Bukhsh, M. Ali, *Eur. J. Inorg. Chem.* **2013**, 34, 5854–5861.

Received: August 14, 2014

Published Online: November 26, 2014